

---

# APPLICATION OF CaCO<sub>3</sub>-NANOPARTICLES FOR CONSOLIDATION OF DAMAGED COPTIC PLASTERS IN EGYPT

Hussein Marey Mahmoud<sup>1\*</sup> and Ayman El-Midany<sup>2</sup>

<sup>1</sup> Cairo University, Faculty of Archaeology, Department of Conservation, 12613 Giza, Egypt.

<sup>2</sup> Cairo University, Faculty of Engineering, Department of Mining, Petroleum and Metallurgy, 12613 Giza, Egypt

(Received 9 September 2012, revised 17 March 2013)

---

## Abstract

Egypt has the largest fortune of cultural heritage materials of different kinds which record the history of the Egyptian civilization. These materials are subjected to different deterioration factors causing several damages to the inner matrix as well as disfiguring the appearance of these materials. The present study aims to prepare and evaluate CaCO<sub>3</sub>-nanoparticles to consolidate damaged Coptic plasters collected from the monastery of Saint Simeon (Deir Anba Hatre), Aswan, Upper Egypt. The evaluation of the consolidation process was performed using scanning electron microscopy (SEM) in addition to measuring the physical and mechanical properties of the samples. The obtained results showed that the consolidation with CaCO<sub>3</sub>-nanoparticles was beneficial in improving the physical and mechanical properties of the treated samples.

*Keywords:* Coptic plasters, Saint Simeon Monastery, CaCO<sub>3</sub>-nanoparticles, Consolidation, SEM-EDS

---

## 1. Introduction

### 1.1. The monastery of Saint Simeon

The monastery of Saint Simeon is located one thousand two hundred meters from the west bank oppose the southern tip of the island of Elephantine (Figure 1). The original name of this monastery is Anba Hatre, it was named after an anchorite who was consecrated as bishop of Syene (now Aswan), by Patriarch Theophilus (385–412 AD). This monastery is located on the west bank of the Nile, opposite of Aswan. The first signs of this monastery are from the 6<sup>th</sup> or 7<sup>th</sup> century. Significant building activity came in the 11<sup>th</sup> century. The monastery was significantly damaged by Salah al-Din (Saladin) in the 12<sup>th</sup> century. By the end of the 13<sup>th</sup> century, the monastery had been abandoned [1]. Even though much of the monastery is in ruins, many of its main features are

---

\* E-mail: marai79@hotmail.com

well preserved. It is of considerable architectural interest, for the church provides the most important example of an oblong, domed Christian church in Egypt and the keep, or tower, which served as a permanent residential complex, is the most developed of its kind. The principal Church of the Monastery, the refectory, and a few damaged wall paintings that are believed to very antiquated, perhaps as old as the 11<sup>th</sup> century [2; J. Dunn, *St. Simeon monastery (monastery of Anba Hatre)*, <http://www.touregypt.net/featurestories/simeon.htm>].

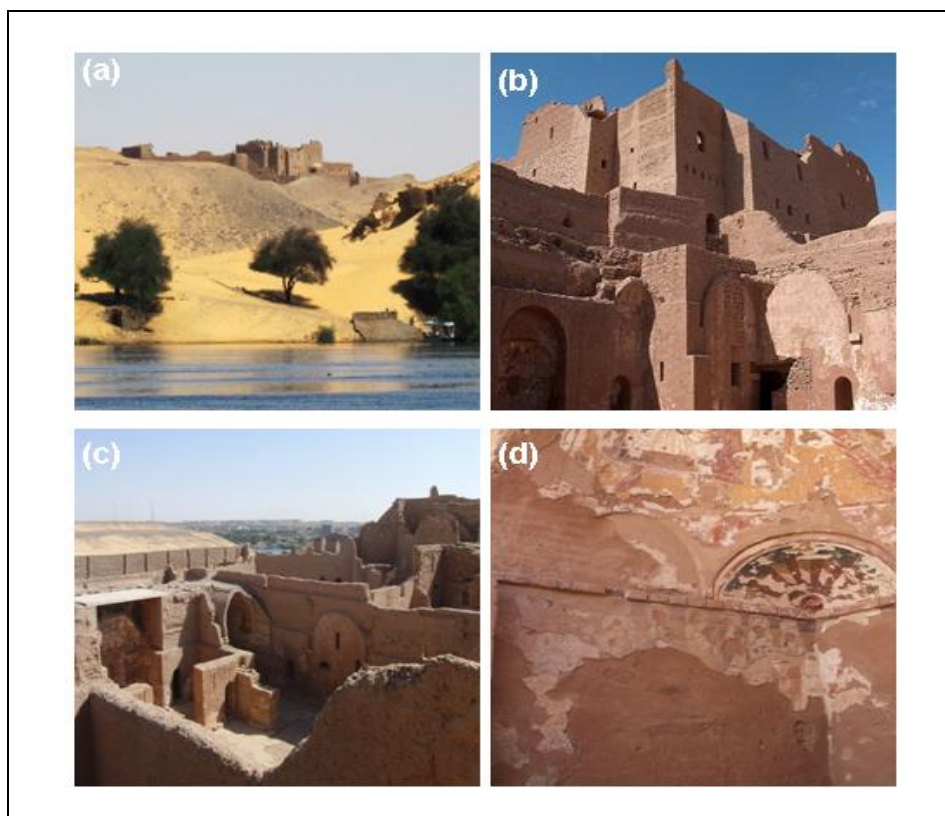


**Figure 1.** (a) general view of the monastery of Saint Simeon (Anba Hatre) at Aswan, (b) towers and ruins of structures at the monastery, (c) ruins of some niches at the monastery, d) wall paintings at the principal church in the monastery.

## 1.2. Nanomaterials

Particles of nanometer sizes began to attract the attention of scientists in different fields in the last two decades. Nanoparticles have been utilized for fabrication of products with desirable characteristics such as higher homogeneity; higher solubility and/or higher strength [3]. They are increasingly used in many areas of chemical and pharmaceutical as well as in ceramic and microelectronic industry [4]. Nanoparticle treatment is the logical evolution of the Ferroni-Dini method. Dispersions of kinetically stable  $\text{Ca}(\text{OH})_2$  nanoparticles in non-aqueous solvents solved most of the drawbacks of the

micro-sized powders. The dispersions of nanoparticles are similar to an extremely concentrated solution of lime water (up to 30% volume fraction), well above the physico-chemical limit imposed by the solubility of calcium hydroxide in water [5]. The polymer provides a carrier environment for the nano-scale materials, and improves the dispersibility and stability of the nano-scale inorganic phase. Organic–inorganic nano-composites can be prepared by directly mixing nano-particles with organic compounds or by a sol-gel process. Commonly used inorganic nano-particles include SiO<sub>2</sub>, TiO<sub>2</sub>, ZnO, and CaCO<sub>3</sub> [6].

### **1.3. Mechanical milling**

Generally known as mechanochemistry or mechanical alloying, is nowadays one of the widely used preparation techniques to obtain nanoparticles [7–9]. The mechanical method avoids lengthy, costly and environmentally sensitive production procedures associated with the solution route. Moreover, it is feasible for large-scale production as well as being simple and low cost [10]. Grinding mills typically used in the process include the attrition jet, planetary, oscillating and vibration mills, all of which are classified as high-energy mills. The high energy ball mills most commonly used in research laboratories comprise one or more containers in which the powder and balls are placed. High energy ball mills, in which the balls are in permanent relative motion, differ from the mills traditionally used in industry to grind materials in either dry or wet conditions. Low energy mills can be used to fabricate certain materials by mechanosynthesis, but the milling time then becomes excessively long, from a few hundred to a thousand hours, which significantly reduces their industrial potential, compared with process times of a few hours or a few tens of hours for high energy mills. However, the production capacity of high energy mills needs to be adapted to suit industrial requirements. Among the above mentioned high-energy mills, the planetary mill is an efficient and suitable device for the production of nanoparticles. As its name implies, the milling container is rotated about two separate parallel axes in a manner analogous to the revolution of a planet around the sun. Comminution processes using laboratory batch planetary ball mills have been reported by many authors [11–15]. Therefore, in the current study the planetary ball mill will be used for the preparation of silica and calcium carbonate nanoparticles for archaeological stones conservation.

## **2. Experimental**

### **2.1. Materials**

The carbonate stone samples were obtained from El-Qurna Locality (670 km south of the city of Cairo). This formation is composed mainly of a marine limestone (lower Eocene).

## 2.2. Analytical techniques

### 2.2.1. Scanning electron microscopy with an EDS microanalysis detector (SEM)

The morphological characteristics of the archaeological and laboratory samples were determined by a JEOL JSM-840A scanning electron microscope. The accelerating voltage 20 kV, probe current 45 nA, the working distance 20 mm and the counting time 60s real time. The matrix correction protocol was ZAF correction. The samples were coated with carbon, using a Jeol JEE-4X vacuum evaporator.

### 2.2.2. X-ray diffraction analysis (XRD)

XRD analysis was performed using a Phillips PW1840 diffractometer with Ni-filtered Cu-K $\alpha$  radiation. The samples were scanned over the 3–63 °2 $\theta$  interval at a scanning speed of 1.2°/min. The detection limit was  $\pm 2$  % w/w.

### 2.2.3. Determination of basic physical properties

For the determination of basic physical properties, the archaeological and laboratory samples were dried in an oven at to constant weight. These weight measurements were recorded as the dry weights of the samples ( $m_{dry}$ ). The saturation of samples in water was carried out in a vacuum oven (Lab-line 3608-6CE Vacuum Oven). The weights of the water-saturated samples were recorded as saturated weights ( $m_{sat}$ ). The weight of saturated samples was also measured in water and recorded as the Archimedes weight ( $m_{arch}$ ) of the samples. All weights were measured with the sensitivity of 0.01g and they were used in the calculation of the porosity and density of the sample. Then, vales of porosity, apparent density, real density and capillary water absorption were measured as recommended by RILEM [16].

### 2.2.4. Determination of Uniaxial Compressive Strength

The determination of Uniaxial Compressive Strengths of bricks and mortars were measured by Shimadizu AG-I Mechanical Test Instrument. Samples were prepared by using a cutting machine (Discoplan-TS 372). The lumps of collected samples were cut into pieces with prismatic shapes with the minimum thickness of 30mm. Shimadzu AG-I Mechanical Test Instrument automatically computed, displayed and recorded test results using a software system. Maximum 15 kN force was applied with 1mm/min. speed. The strokes were recorded under loading. The relationship between the strokes and load by a graph was automatically displayed on the test condition monitor. This graph was composed of a curve whose peak point gave the 34 maximum force (F) under which the specimen failed. As a result, uniaxial compressive strengths

represented by 'σ' were calculated by using this graph with the following formula:

$$\sigma = F/A \quad (1)$$

where;

F: failure load (kN)

A: area onto which loading was applied (mm<sup>2</sup>).

### **3. Results**

#### ***3.1. Characterization of the archaeological plasters***

##### *3.1.1. Morphological and microanalysis*

SEM image obtained on the lime plasters samples shows the porous lime matrix and the aggregates used in the plasters are mostly semi-rounded (Figure 2). The microanalysis on the sample shows EDS signals of Ca, C and O for calcium carbonate, while the small peaks of Si, Fe and Al indicates the contribution of aluminosilicate materials (e.g. clays).

##### *3.1.2. Mineralogical characterization*

XRD analysis of the plaster samples showed that calcite (CaCO<sub>3</sub>) is the main component with traces of potassium feldspar (microcline, KAlSi<sub>3</sub>O<sub>8</sub>), plagioclase (albite, NaAlSi<sub>3</sub>O<sub>8</sub>) and kaolinite (Al<sub>2</sub>Si<sub>2</sub>O<sub>5</sub>(OH)<sub>4</sub>).

##### *3.1.3. Basic physical and mechanical properties of mortar samples*

The porosity values of the plasters were in the range of 37–39 % and their average value was 34 %. The real density values of them were 1.1–1.4 g/cm<sup>3</sup>. Their apparent density values ranged between 1.2–1.5 g/cm<sup>3</sup>. Dry Compressive strength values were of average of 6.4 MPa. Ultimate strength values of the samples were 6.5 and 8.3 MPa. Modulus of elasticity values were 100 MPa and 110 MPa, yield strength values of 2.6 and 3 MPa.

#### ***3.2. Preparation of nano-calcium carbonates***

Nano calcium carbonates particles were produced by milling in a Fritsch Pulverisette P5 Planetary ball mill with wear resistant commercially available zircon oxide (ZrO<sub>2</sub>) milling beads in the sized range of 0.5 mm (Fritsch, Germany). The ball to powder ratio was kept at 4:1. The milling was carried out at 350 rpm for milling different times. Milled samples were retrieved at suitable intervals for characterization. The cyclosizer for sub-sieve sizing was used for particle size distribution analysis.

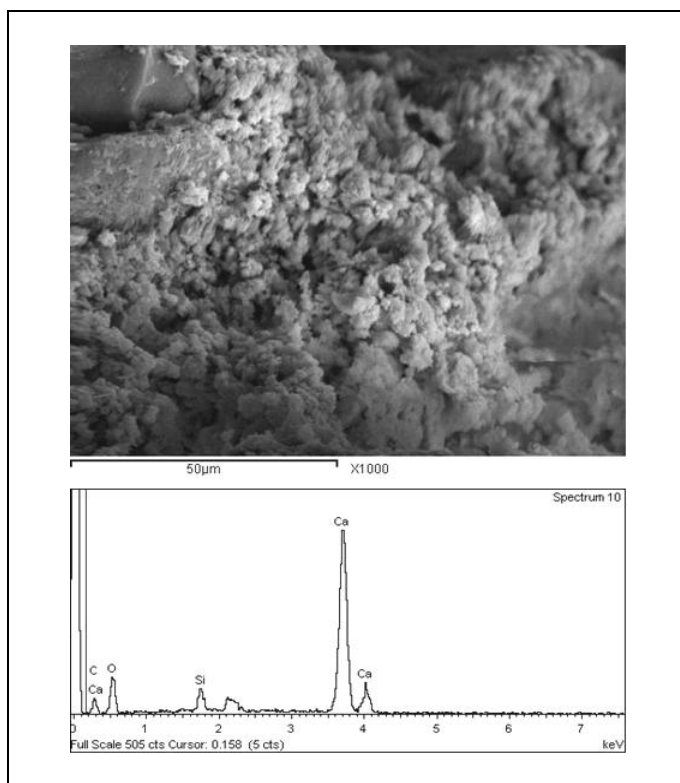


**Figure 2.** (up) SEM micrograph of the damaged plaster sample, (down) EDS spectrum of obtained on the sample.

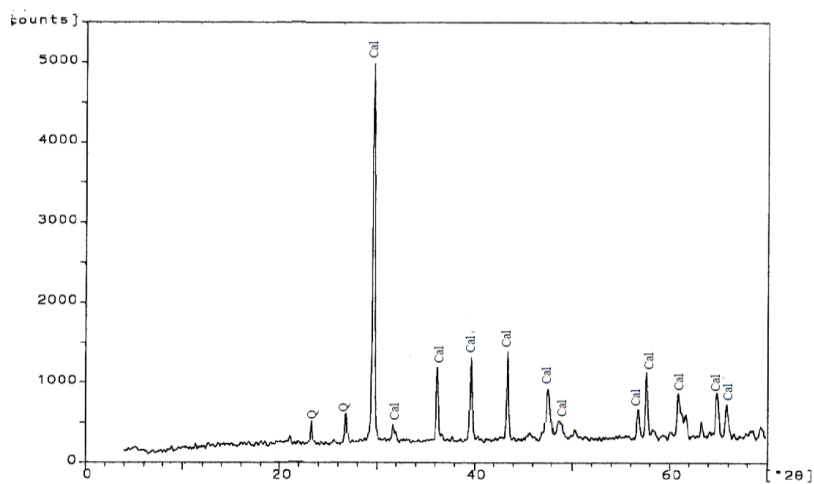


**Figure 3.** XRD pattern of the prepared nano-CaCO<sub>3</sub>.

### 3.2.1. Determination of nano-CaCO<sub>3</sub> by EDS and XRD analyses

EDS microanalysis of the nano-CaCO<sub>3</sub> samples shows that calcium is the major ion contained, while silicon, aluminium, iron and titanium were also measured. XRD analysis confirmed calcite as the major component in the samples with traces of quartz (Figure 3). The results affirmed that the grinding did not change the chemical and mineralogical composition of the samples (Table 1).

**Table 1.** Chemical analysis of the nano-CaCO<sub>3</sub>.

Atomic (%)		Compound (%)	
Al	0.81	Al <sub>2</sub> O <sub>3</sub>	1.45
Si	1.58	SiO <sub>2</sub>	3.35
Ca	49.85	CaO	92.64
Fe	0.17	Fe <sub>2</sub> O <sub>3</sub>	0.49
Ti	0.16	TiO <sub>2</sub>	0.44
O	47.43	<b>Total = 98.37</b>	
<b>Total</b>	<b>100.00</b>		

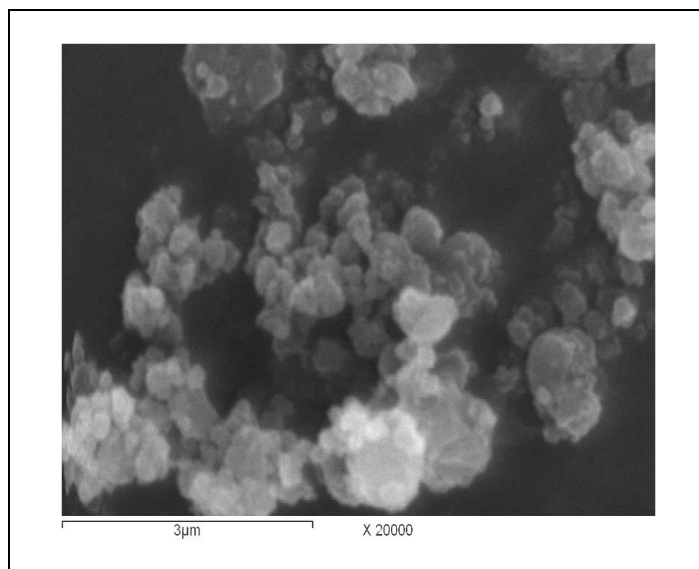


**Figure 4.** SEM micrograph of the prepared nano-CaCO<sub>3</sub>.

### 3.2.2. Determination of nano particle size by SEM

The procedure for preparation of the sample is as follows. The reaction mixture was sprayed on a thin film of methanol on a glass plate and was dried

under atmospheric conditions until all the solvent was evaporated. The residue was washed with methanol several times to remove the surfactant [17]. The sample was dried again under atmospheric conditions till all the solvent was evaporated. The glass plate was then inserted in the SEM to obtain the images. The diameter of the individual particle was calculated from the surface area assuming the particles to be spherical. The nano-CaCO<sub>3</sub> particle size distribution is based on an average of 100 particles measured during the analysis (Figure 4). It is noticed that the particle size is very fine where about 60% of the sample is located in -11 μm size range.

### 3.2.3. Particle size distribution analysis

The cyclosizer was used to conduct the size analysis of the sample due to its fineness. It is noticed that the particle size is very fine where about 60% of the sample is located in -11 mm size range, Table 2.

**Table 2.** Size analysis of the carbonate sample.

Size (μm)	Wt. (%)	Cumulative Wt. (%)
+ 44	14.18	14.18
+ 35	1.81	15.99
+25	6.80	22.79
+15	9.51	32.30
+11	7.92	40.22
-11	59.78	100.00

### 3.2.4. The consolidation of damaged plasters with nano-CaCO<sub>3</sub>

To evaluate the effectiveness of the prepared nano-CaCO<sub>3</sub> on consolidation of the inner matrix of ancient damaged plasters, a dispersion of 5 gL<sup>-1</sup> nano-CaCO<sub>3</sub> in 2-propanol was applied for several times by brush on the samples' surfaces to insure a good wettability. The distribution of the nano-CaCO<sub>3</sub> particles into the inner matrix of the plasters is approximately uniform. The CaCO<sub>3</sub> nanoparticles showed a good penetration through the pore network of the samples. The higher carbonatation efficiency is confirmed by a SEM micrograph obtained on the plaster sample after application of nano-CaCO<sub>3</sub> (Figure 5) which shows the formation of new calcite crystals in deep zones in the samples (about 30 mm from the outer surface). EDS microanalysis obtained after the treatment (Figure 5 down) shows the high amount of calcium in the samples suggests high carbonization process occurred after the application of CaCO<sub>3</sub> nanoparticles. The apparent density values after treatment ranged between 1.3–1.6 g/cm<sup>3</sup>. The real density values of them were 2.6–2.8 g/cm<sup>3</sup>. The porosity values of the treated mortars were in the range of 22% and water

absorption was of 34%. After treatment, dry compressive strength values were of average of 7.2 MPa. Ultimate strength values of the samples were 7.8 and 9.2 MPa. Modulus of elasticity values were 113 MPa and 119 MPa, yield strength values of 2.9 and 4.1 MPa.

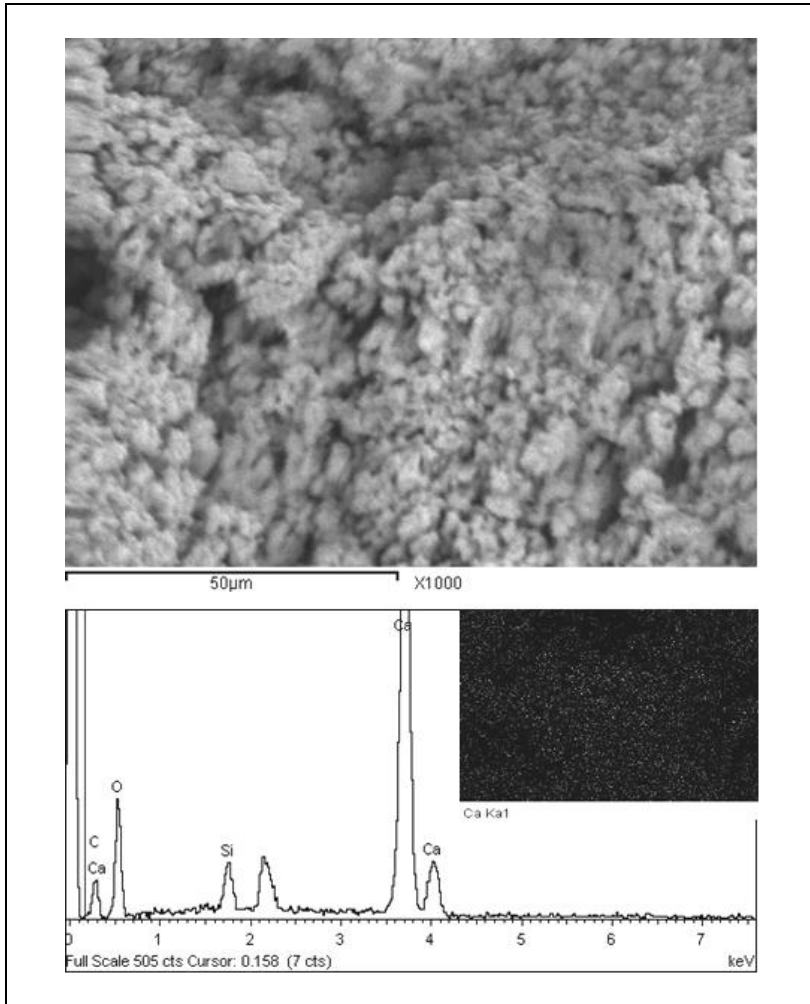


**Figure 5.** (up) SEM micrograph of the plaster samples after the application of CaCO<sub>3</sub> nanoparticles, (down) EDS spectrum of lime-plaster sample.

#### **4. Conclusions**

The aim of this work was to investigate the application of CaCO<sub>3</sub>-nanoparticles, obtained by mechanical milling process, for the consolidation of Coptic plasters collected from the monastery of Saint Simeon (Deir Anba Hatre), Aswan, Upper Egypt. The evaluation of the consolidation process was performed via SEM and measuring the physical and mechanical properties of the samples. The obtained results showed that the use of CaCO<sub>3</sub>-nanoparticles was

beneficial in improving the physical and mechanical characteristics of the treated samples and this mainly attributed to the positive effects of CaCO<sub>3</sub>-nanoparticles in terms of strength and acceleration of hydration rate.

## Acknowledgement

This study is a part of project entitled 'Evaluation of some nanomaterials utilization for the safeguard of the cultural heritage in Egypt' funded by Cairo University (The General Administration of Scientific Research).

## References

- [1] R.S. Bagnall and D.W. Rathbone (eds.), *Egypt from Alexander to the Early Christians: An Archaeological and Historical Guide*, Getty Publications, Los Angeles, 2004, 242.
- [2] P. Grossmann, *The Coptic encyclopedia*, A.S. Atiya (ed.), vol. 3, Macmillan, New York, 1991, 851.
- [3] J.A. Hubbell, S.N. Thomas and M.A. Swartz, *Nature*, **462** (2009) 461.
- [4] S. Mende, F. Stenger, W. Peukert and J. Schwedes, *J. Mat. Sci.*, **39** (2004) 5223.
- [5] P. Baglioni, E. Carretti, L. Dei and R. Giorgi, *Nanotechnology for wall paintings conservation, in Self-Assembly*, B.H. Robinson (ed.), IOS press, Amsterdam, 2003, 32-41.
- [6] A. Gupta and P. Dhuri, *Mater. Sci. Eng. A.*, **304-306** (2001) 394.
- [7] B.S. Murthy, M. Mohan Rao and R. Ranganathan, *Acta Metall. Mater.*, **43** (1995) 2443.
- [8] C.N. Chinnasamy, A. Narayanasamy, N. Ponpandian, K. Chattopadhyay and M. Saravana Kumar, *Mater. Sci. Eng., A.*, **304-306** (2001) 408.
- [9] A. Munitz, G. Kimmel, J.C. Rawers and R.J. Fields, *Nanostruct. Mater.*, **8** (1997) 867.
- [10] K. Tokumitsu, *Solid State Ionics*, **101** (1997) 25.
- [11] G.F. Goya, *J. Matter. Sci.*, **39** (2004) 5045.
- [12] J. Xianjin, A.M. Trunov, M. Schoenitz, R.N. Dave and E.L. Dreizin, *J. Alloys Compd.*, **478** (2009) 246.
- [13] D. Chen, S. Ni and Z. Chen, *China Particuol.*, **5** (2007) 357.
- [14] E.C. Sanchez, E. Torres, C. Diaz, and F. Saito, *J. Mater. Process. Techn.*, **152** (2004) 284.
- [15] L.C. Sanshez, J.D. Arboleda, C. Saragovi, R.D. Zysler and C.A. Barrero, *Physica B*, **389** (2007) 145.
- [16] RILEM, *Materials and Structures*, **13(78)** (1980) 431.
- [17] L. Mathew, and S.K. Narayanankutty, *Synthesis and characterisation of nanosilica*, Proc. of International Conference on Advances in Polymer Technology, Cochin University of Science and Technology, Kerala 2010, 279-284.